Nur Amalina Ramli[1]

Fatmawati Adam[1,2,*]

Noor Fitrah Abu Bakar[3]

Michael E. Ries[4]

Mechanical and Thermal Evaluation of Carrageenan Biocomposite Incorporated with Modified Starch Corroborated by Molecular Interaction Recognition

Vegetarian hard capsule has attracted surging demand as an alternative to gelatin; however, having limited supply. Carrageenan extracted from seaweed has the potential to be utilized as a hard capsule material. Improving the mechanical and thermal properties of carrageenan biocomposite is therefore of great importance for future use in drug delivery system. Hence, carboxymethyl sago starch (CMSS) was incorporated to strengthen the carrageenan biocomposite at concentrations ranging from 0 to 1.0%. The intermolecular hydrogen bonding formed between carrageenan and CMSS was revealed via density functional theory (DFT) calculations and substantiated by ^{1}H NMR and FTIR spectra. The result showed that the hydrogen bond is established between hydroxyl (carrageenan)-carbonyl (CMSS) groups at a distance of 1.87 Å. The bond formation subsequently increased the tensile strength of the biocomposite film and the loop strength of the hard capsule to 64.5 MPa and 40.5 N, respectively. The glass transition temperature of the film was raised from 37.8°C to 47.8°C, increasing the thermal stability. The activation energy of the film is 74.4 kJ·mol^{-1}, representing a 26.2% increase over the control carrageenan. These findings demonstrate that incorporation of CMSS increases the properties of carrageenan biocomposite and provides a promising alternative to animal-based hard capsule.

Keywords:

Activation energy; carrageenan; density functional theory; hard capsule; hydrogen bonding

Author affiliations

[1]Faculty of Chemical & Process Engineering Technology, Universiti Malaysia Pahang, 26300 Kuantan, Pahang, Malaysia.

[2]Centre for Research in Advanced Fluid & Processes, Universiti Malaysia Pahang, 26300 Kuantan, Pahang, Malaysia.

[3]School of Chemical Engineering, College of Engineering, Universiti Teknologi MARA, 40450, Shah Alam, Selangor, Malaysia

[4]School of Physics & Astronomy, University of Leeds, Leeds, United Kingdom

Email corresponding author: fatmawati@ump.edu.my

1 Introduction

Gelatin is widely used for various pharmaceutical dosage forms attributed to its good film-forming properties. The current technology, which uses gelatin as the excipient in producing hard capsules, remains unchanged till now. However, gelatin capsules possess several shortcomings, such as being an animal-derived material. This restricts its consumption for parts of the community due to religious, cultural and vegetarian dietary requirements [1]. This issue influences consumers' preferences for the source of medications, leading to an increased attempt to discover a plant-based alternative. Carrageenan offers valuable properties in gelling, thickening, emulsifying and stabilising functions that have ensured its applications and market demand in the pharmaceutical industry [2–4]. Despite that, carrageenan film has low mechanical strength, which limits its potential application [5,6]. It becomes brittle after drying due to the formation of double helices in the carrageenan matrix [7,8]. Therefore, several chemical modifications have been investigated in order to improve the mechanical properties of carrageenan in the preparation of hard capsules, such as incorporation with carboxymethyl cellulose (CMC) and microcrystalline cellulose

(MCC) [9,10], cellulose nanocrystals (CNC) [5], isovanillin [11] and Arabic gum [12]. In a separate study, Zainal Abedin and Abu Bakar demonstrated that Tween 20 and Tween 40 emulsifiers significantly improved the tensile strength of the carrageenan films from 7.35 to 13.83 MPa [13]. Another approach, conducted by Abdul Khalil [14], found that carrageenan film blended with corn starch at a ratio of 90:10 increased the tensile strength from 72.9 MPa to 77.0 MPa. The establishment of hydrogen bond interactions between carrageenan and crosslinker or filler affects the matrix arrangement, thus changing the biocomposite properties [15]. The ability of a film-based product to withstand mechanical damage with an appropriate level of flexibility for easy handling and processing is an important feature in its development [16].

Plant-based hard capsules made of hydroxypropylmethyl cellulose (HPMC) are available on the market, but at a higher price than gelatin [17]. A cost-cutting strategy would be to blend HPMC with a lower-priced thickening agent. Starch, a plant-based and sustainable material, has piqued the interest of researchers who want to emphasise its functions in various dosage forms [18]. Starch is a well-known natural hydrophilic polymer found in many staple foods. Malaysia is the world's third largest sago producer, with 67,957 hectares of sago-cultivated land in Sarawak [19,20]. Sago starch can be extracted from sago palms (Metroxylon sago) [21]. Among starch derivatives, carboxymethyl starch (CMS) has received considerable attention recently, specifically in drug delivery applications [22]. Derivatisation of starch, which carries negatively charged functional groups (CH_2COO^-), provides a unique characteristic for CMS as a pH-responsive excipient. The carboxymethyl polar groups bound to the hydroxyl groups of CMS are responsible for its adsorption behaviour, which increases the swelling and water solubility of the starch [21,23]. Research on carboxymethyl derivatives mostly leans towards carboxymethyl cellulose (CMC) [24]. On the other hand, CMS could also be utilised to develop edible films by blending with other materials, and further research in this area is needed.

The current work aims to study the possible intermolecular interaction between carrageenan and CMSS in improving the properties of the biocomposite with incorporation of an optimal amount of CMSS blending with HPMC. Carrageenan biocomposite with the inclusion of HPMC was proven to increase the tensile strength and the thermal activation energy up to 56% and 43%, respectively [25]. The mechanical and thermal properties of the hard capsule are hypothesised to be enhanced due to the formation of intermolecular hydrogen bonding between carrageenan and CMSS. The formation of hydrogen bonds is a key component of chemical structure, conformation, and reactivity [26–28]. Thus, detection of hydrogen bonding remains an active area of research. DFT calculation and NMR spectroscopy are included among the most effective tools to investigate and to provide evidence of interaction mechanism in theoretical and experimental studies. Fig. 1 represents the preparation method of carrageenan hard capsules and the proposed hydrogen bonding interaction between carrageenan and CMSS. By improving the mechanical and thermal properties of the carrageenan biocomposite, the as-prepared capsules will have the potential to be an alternative to gelatin capsules.

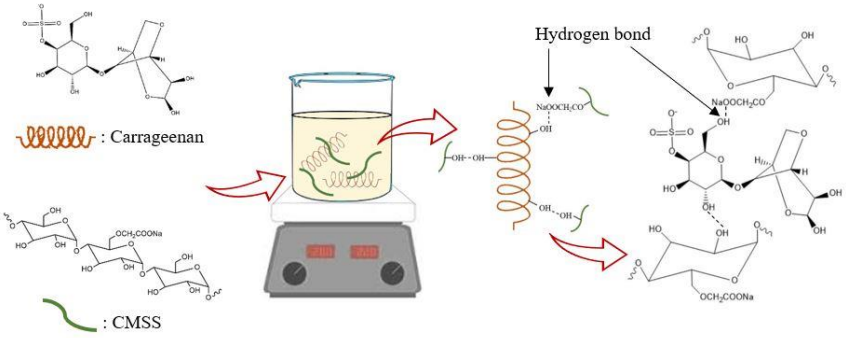

Figure 1 Schematic representation of the preparation of Carra-CMSS biocomposite and the intermolecular hydrogen bonding interaction between both materials.

2 Materials and Methods

2.1 Materials

Refined carrageenan was purchased from CV Simpul Agro Globalindo, Indonesia (molecular weight ranges from 930 to 1010 g/mol with 31.5% carbon, 5.97% hydrogen, 0% nitrogen, and 6.28% sulphur) [11]. Carboxymethyl sago starch (CMSS) was purchased from My Synergy Factors (M) Sdn. Bhd., Malaysia. Hydroxypropylmethyl cellulose (HPMC) (molecular weight of 86 kDa), anise (methoxybenzyl alcohol, 98%) and calcium alginic acid (molecular weight of 584.4 Da) were purchased from Sigma-Aldrich, (USA). Polyethylene glycol (PEG) (molecular weight of 400 Da) as a plasticiser was purchased from Merck (Germany). All chemicals used are of analytical grade.

2.2 Quantum Mechanics Simulation

Molecular dynamic software, Gaussian 09W was executed to simulate the intermolecular interaction between κ-carrageenan and CMSS. The geometries of all molecules were optimized via DFT calculations using B3LYP functional with 6-31G (d,p) basis set [29]. The molecular electronic surface potential (MESP) of κ-carrageenan and CMSS were generated from the geometry-optimized calculation. The quantum mechanics evaluation has been used to calculate the interaction energy and the enthalpy formation of the hydrogen bond using Eq. 1 and Eq. 2, respectively.

$$\text{Interaction energy} = \mathrm{E_{SCF\ complex}} - \left(\mathrm{E_{SCF\ carrageenan}} + \mathrm{E_{SCF\ CMSS}}\right) \quad (1)$$

$$\Delta \mathrm{H_{formation}} = \mathrm{H_{complex}} - \left(\mathrm{H_{carrageenan}} + \mathrm{H_{CMSS}}\right) \quad (2)$$

2.3 Preparation of Carra-HPMC/CMSS Biocomposite Film and Hard Capsules

A range of CMSS concentrations (0 to 1.0% w/v), was added to 2% w/v refined carrageenan in 150 ml deionised water at 60°C. HPMC at a fixed concentration was added beforehand. Anise and calcium alginic acid were also mixed in the formulation as a crosslinker and toughening agent, respectively. 20 mL of solution was poured into a stainless-steel tray after 3 hours of mixing before it was dried overnight at room temperature for film making. Meanwhile the other portion of the solution was dipped using capsule pins of size "1" to prepare hard capsules. Dry films and hard capsules were then employed for characterisation and analysis.

2.4 ^{1}H-NMR Spectroscopy Analysis

The 500 MHz of ^{1}H NMR spectra were recorded using an NMR spectrometer (Bruker Ultra Shield Plus, Germany) which was operated at room temperature. Samples were prepared at a concentration of 10 mg/ml in deuterated water (D_2O) before it is transferred into the NMR tube. The chemical shifts were measured in respect to the remaining proton resonance of D_2O (δ = 4.70 ppm).

2.5 FTIR Spectroscopy Analysis

FTIR analysis was conducted using the ATR-FTIR spectrometer (Perkin Elmer, USA) to examine the chemical bonding between carrageenan and CMSS. FTIR spectra of raw materials and the prepared films were measured between 400 and 4000 cm^{-1}. A total of 16 scans were obtained at 0.15 s/scan and a spectral resolution of 8 cm^{-1}.

2.6 Viscosity Measurement

The viscosity of carrageenan biocomposite solution was measured using a rotational rheometer (Rheo 3000, USA) equipped with LCT 25 4000010 geometry. Approximately 15 mL of the biocomposite solution was filled into the measuring tube. The measurement was programmed at a speed of 300 revolutions per minute, with 100 MPoints at a pre-heated temperature of 40°C.

2.7 Mechanical Properties Analysis

The tensile strength and elongation at break of 2 cm x 6 cm of carrageenan film strips were calculated using a texture analyser (CT3, USA) equipped with TexturePro CT V1-8 Build 3.1 and fitted with a load cell of 5 kN. The analyser was operated with an initial grip separation of 30 mm and a crosshead speed of 30 mm min^{-1}. The hard capsule loop test was also performed using the texture analyser (CT3, USA). The instrument was fitted with two separated rod fixtures. The upper fixture protruded horizontally from the set location with a target value of 5.0 mm at a fixed speed of 0.50 mm/s. The force applied to break the hard capsule was recorded.

2.8 Moisture Content Analysis

The moisture content of the film was determined using a moisture analyser (MS70, A&D, Japan). Approximately 0.1 g of the sample was placed at the top of the heating pan. The moisture content was determined by the reduction in sample mass until it reached a constant value after heated-air drying.

2.9 Disintegration Test

A disintegration test was carried out using a disintegration tester (Distek 3100, Germany) following USP-701. The capsules were inserted in tubes and then plunged into 600 mL of distilled water at 37°C ± 2°C. The capsules were filled with lactose placebo. The time (min) taken for the lactose to initially diffuse from the capsules into the medium was recorded as the capsule disintegration time.

2.10 Morphological Analysis

Scanning electron microscope (S26000-N Hitachi, Japan) was used to observe the surface morphology of carrageenan film below 5000x magnification. To determine the transparency of the film, the opacity of the film was measured. The films were cut into 3 cm × 0.3 cm rectangles and laid in the cuvette. The spectrophotometer was set to 600 nm to measure the opacity of the film using Eq. 3 [30] as follows;

$$\text{Opacity} = \frac{\text{Abs } 600}{\text{b}} \tag{3}$$

where Abs 600 is the absorbance value at 600 nm, and b is the film thickness (mm).

2.11 Thermal Stability Analysis

In a nitrogen atmosphere, about 3 mg of the sample was heated at 10°C/min from 30°C to 400°C for differential thermal analysis. The thermograms collected by a differential scanning calorimeter (DSC) (Polyma214, Germany) were used to determine the glass transition, melting, and crystallisation temperatures. Thermal properties in terms of mass loss of carrageenan films were then analysed using thermogravimetric analysis (STA7200 Hitachi, Japan) where approximately 3 mg of film was heated at 10°C/min from 30°C to 700°C in the airflow.

2.12 Kinetic Analysis

Activation energy (E_a) for the main stage of decomposition was calculated on the basis of TGA analysis and Arrhenius kinetic theory. It was calculated from the slope of the plot of ln [ln (1/y)] versus 1000/T [31,32], which yielded a straight line based on Broido's equation, as in Eq. 4:

$$\ln\left[\ln\left(\frac{1}{\text{y}}\right)\right] = -\left(\frac{\text{Ea}}{\text{RT}}\right) + \ln \text{A} \tag{4}$$

where, E_a is the activation energy (kJ/mol), R is the universal gas constant (R = 8.314 $J{\cdot}mol^{-1}{\cdot}K^{-1}$), T is the temperature recorded in thermogram (K), and A is the pre-exponential factor (min^{-1}). The conversion degree was calculated using Eq. 5:

$$\text{y} = \frac{\text{wt} - \text{w}\infty}{\text{wo} - \text{w}\infty} \tag{5}$$

where the degree of conversion is denoted by y, w_t is the weight at any time (fraction that has not yet decomposed), w_o is the initial weight, and w_∞ is the weight of residue.

2.13 Statistical Analysis

All data were reported as the mean ± standard deviation of three different repetitions. A one-way variance analysis (ANOVA) was used to measure the confidence level of the p-value, which was found statistically significant by $p<0.05$. The testing of null analysis (H_o) and alternate analysis (H_i) was carried out for viscosity, tensile strength, elongation at break, capsule loop strength, moisture content, and disintegration time of Carra-HPMC/CMSS biocomposite film and hard capsules.

3 Results and Discussion

3.1 Quantum Mechanics Simulation

The charge distribution of κ-carrageenan and CMSS in Fig. 2 was illustrated from the optimized MESP. The electron potential increases according to the electron density in an order of blue<green<yellow<orange<red [29]. Based on the Mulliken charge, Region I (oxygen atom) in carrageenan was generated with red colour as the most negative electrostatic potential. While the blue color of Region IV (sodium atom) in CMSS represented the most positive electrostatic potential. Therefore, both of these regions may interact and form intermolecular hydrogen bond. There are possibilities of the hydrogen bond to form between different functional groups as shown in the optimization of the κ-carrageenan-CMSS conjugate (Fig.3). A hydrogen bond (87H---115O) was established between hydrogen atom of κ-carrageenan (Region II) and carbonyl group of CMSS (Region III) with a distance of 1.87Å (Fig. 3). The hydrogen bond length established for κ-carrageenan and isovanilin is around 1.74 to 1.79 Å [11], while between κ-carrageenan and glyoxylic acid is with a bond length of 1.90 Å [29]. The Mulliken atomic charge of 87H atom in Region II is 0.32 and 115O atom in Region III is -0.59. The bond formed between both regions is due to the difference in electron density. The calculated interaction energy and enthalpy formation of the hydrogen bond between κ-carrageenan-CMSS using Eq. 1 and Eq. 2 are −97,826.1 and 60.9 kJ·mol^{-1}, respectively (Table 1). The large interaction energy and enthalpy formation values of the conjugate are due to the presence of strong intermolecular hydrogen bond interaction [33]. These indicate the compatibility of κ-carrageenan-CMSS conjugate through hydrogen bond formation, which contribute to the potential of CMSS to be used in the development of carrageenan hard capsule.

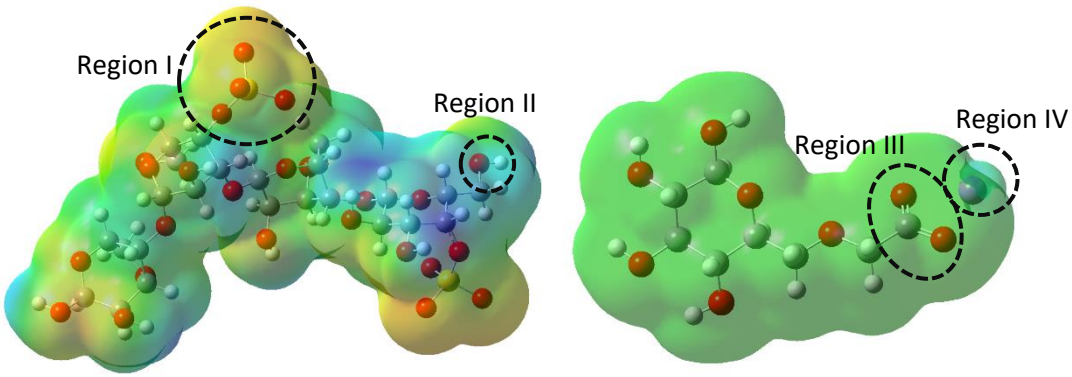

Figure 2 Optimized MESP structure of (a) κ -carrageenan and (b) CMSS.

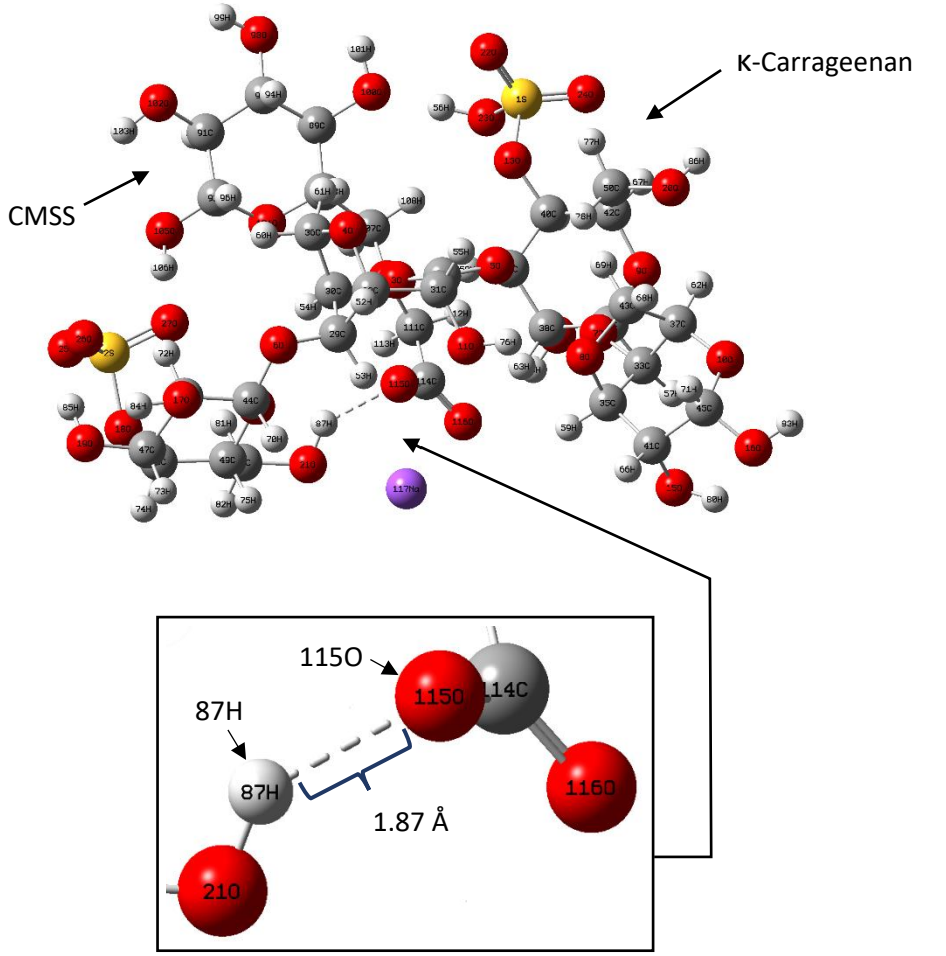

Figure 3 Complex molecular structure of κ-carrageenan-CMSS conjugate.

Table 1 The calculated energies and enthalpies of raw and complex molecular structure of κ-carrageenan-CMSS.

Samples	E_{SCF} (kJ·mol^{-1})	H (kJ·mol^{-1})
Carrageenan	−9,388,131.6	1842.01
CMSS	−2,827,164.7	649.03
Carrageenan-CMSS	−12,313,122.4	2552.03

3.2 ^{1}H-NMR Spectroscopy and Mechanism of Carra-CMSS Biocomposite

Carrageenan and CMSS were subjected to ^{1}H NMR spectroscopy to acquire molecular-level insight into their structures and to further validate the possible intermolecular interactions. The structure of kappa carrageenan can be divided into two units as in Fig. 4(a). G-unit refers to alternating 3-linked β-d-galactopyranose, and DA-unit refers to 4-linked 3,6-anhydro-α-D-galactopyranose [34,35]. The six spectral peaks at G-unit are G1 (1H; 5.02 ppm), G2 (O-2H; 3.59 ppm), G3 (2H; 3.90 ppm), G4 (1H; 4.86 ppm), and G5,6 (O-2H; 3.71 ppm). The DA-unit also has six peaks: DA1 (1H; 4.94 ppm), DA2 (O-2H; 3.99 pm), DA3 (O-1H; 4.30 ppm), DA4 (O-1H; 4.59 ppm), DA5 (1H; 4.62 ppm), and DA6 (2H; 4.10 ppm). The listed spectral peaks are in line with those found by Abu Bakar [36] and Voron'ko [37] with minor differences that could be due to differences in sample preparation and solvent used. The carrageenan was used in this study without any prior treatment.

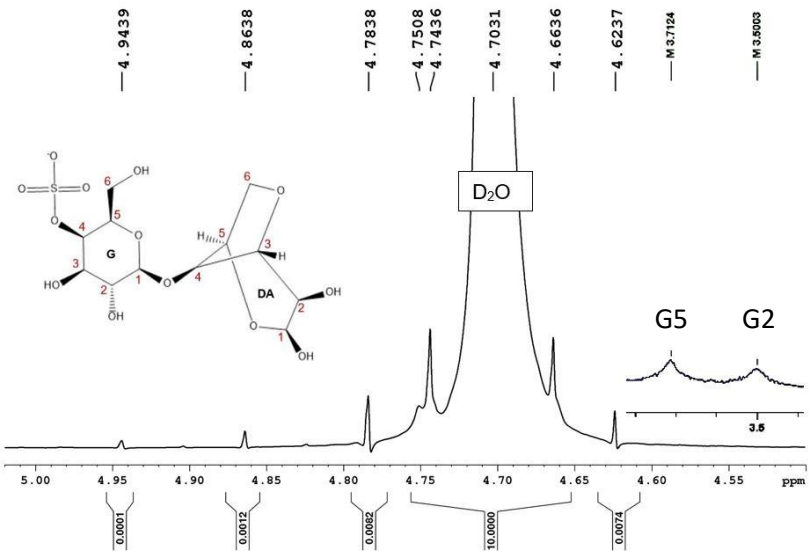

Figure 4(a). ^{1}H-NMR spectrum of pure carrageenan.

Fig. 4(b) depicts the spectrum of pure CMSS. The spectral peaks of anomeric hydrogen (H1), which are ascribed to the proton at C_1 of the α-anomer, are observed in the lower field (5.03 and 4.94 ppm). In the higher field (4.86 and 4.78 ppm), the peaks are assigned to the proton at C_1 of the β-anomer [27,28]. The carboxymethyl (-OCH_2COO^-) protons are detected in the range of 4.0 to 4.5 ppm. The peaks of anhydroglucose unit protons (H2, H3, H4, H5, H6) are represented in between 3.3 and 3.9 ppm, which are within the range reported by Zdanowicz [38].

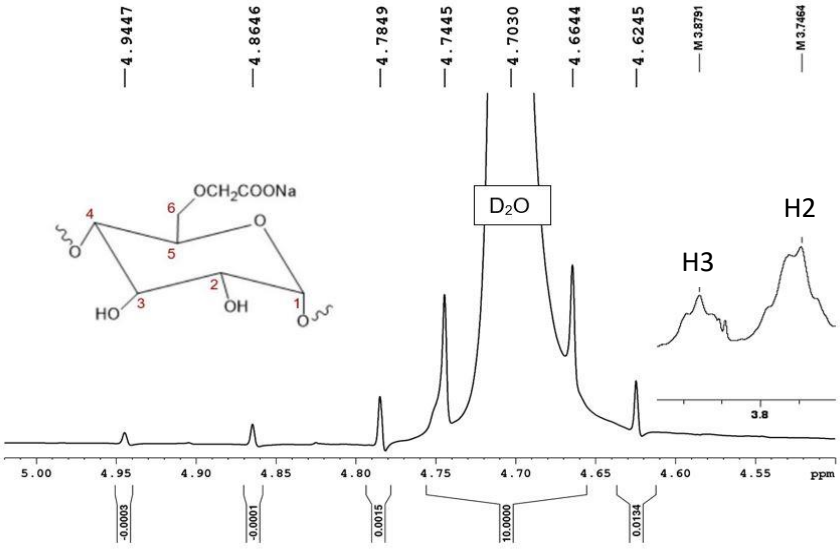

Figure 4(b). ^{1}H-NMR spectrum of pure CMSS.

The NMR spectrum is used to examine the interaction mechanism of hydrogen bonding between carrageenan and CMSS as it demostrates the proton chemical shifts to shield or deshield. Deshielding causes the peaks to shift to a higher frequency when intermolecular hydrogen bonding forms. The electronegativity increases as the peak shifts to the left and becomes further downfield. The chemical shift increases the conjugate molecule's shielding effect by bringing the hydrogen closer to the electronegative atom. In the molecule conjugate, the chemical shifting to the left occurs at two points: G2--H2 and G5--H3 (Fig. 4(c)). At the first bond, the peak G2 of carrageenan shifts from 3.50 to 3.52 ppm while the peak H2 of CMSS shifts from 3.74 to 3.75 ppm (Table 2). Second, the peak G5 of carrageenan deshields to 3.73 ppm from 3.71 while the peak H3 of CMSS deshields to 3.91 ppm from 3.88. These peaks shift to higher frequencies, implying that they require a lower density of external magnetic field to make specific protons

resonant. This is because hydrogen bonding has weakened their magnetic field [39].

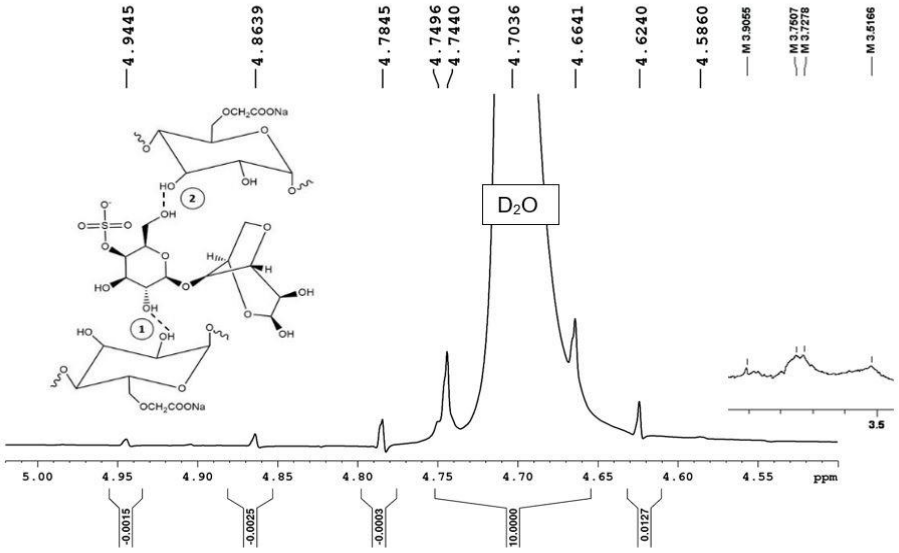

Figure 4(c). ^{1}H-NMR spectra of Carra-CMSS biocomposite.

Table 2. ^{1}H NMR chemical shifts of Carra-CMSS biocomposite.

Samples	Chemical Shifts in Hydrogen Bond 1 (ppm)	Chemical Shifts in Hydrogen Bond 2 (ppm)
Carrageenan	G2 : 3.50	G5 : 3.71
CMSS	H2 : 3.74	H3 : 3.88
Carra-CMSS	G2 : 3.52	G5 : 3.72
	H2 : 3.75	H3 : 3.91

The hydrogen bond proven from ^{1}H NMR is formed in different functional groups when compared to the theoretical DFT calculation. It demonstrates that the hydrogen bond was formed between the hydroxyl groups of carrageenan and CMSS. However, in the simulation, the formation is between the hydroxyl group of carrageenan and carbonyl group of CMSS. Insufficient concentrated sample analysed in room temperature with the choice of solvent might be the limitation that caused to the low senstivity of the ^{1}H NMR technique [26,40]. However, the presence of intermolecular hydrogen bonding, despite of which functional groups interact, plays the pivotal role that can elucidate the potential of CMSS to be used in the carrageenan biocomposite.

3.3 Fourier Transform Infrared Spectroscopy

Fig. 5 shows the spectra of carrageenan, CMSS, and Carra-CMSS biocomposite film. Carrageenan produces distinctive peaks at 1223 cm^{-1} and at 1034 cm^{-1}, indicating the sulphate esters (-SO) and the glycosidic linkage (-CO) of carrageenan, respectively [41][42]. The peak of 3,6-anhydro-D-galactose emerges at 921 cm^{-1} while the peak of C-O-SO_4 on D-galactose-4-sulphate appears at 841 cm^{-1}. The carrageenan spectrum is comparable to the findings from Adam [2], Ili Balqis [43] and Sun [44]. After the addition of CMSS, the carboxymethylation of sago starch gives an additional peak at 1584 cm^{-1} which reflects the substitution of the carboxymethyl ether (-COO-Na^{+}) group on the sago starch chains [39,45,46]. The characteristic of anhydroglucose (-CO) stretching can also be seen. This band is absorbed at 1060 cm^{-1} in the control film and shifts to a lower wavenumber (1042 cm^{-1}) for Carra-CMSS 0.4. It denotes the formation of a more stable hydrogen bond between carrageenan and CMSS. The enhanced intermolecular hydrogen bonding between carrageenan and CMSS is also demonstrated by a shift in the peak of -OH stretching from 3391 cm^{-1} (control) to 3388 cm^{-1} for Carra-CMSS 0.4 (shown in Fig. 5(b)).

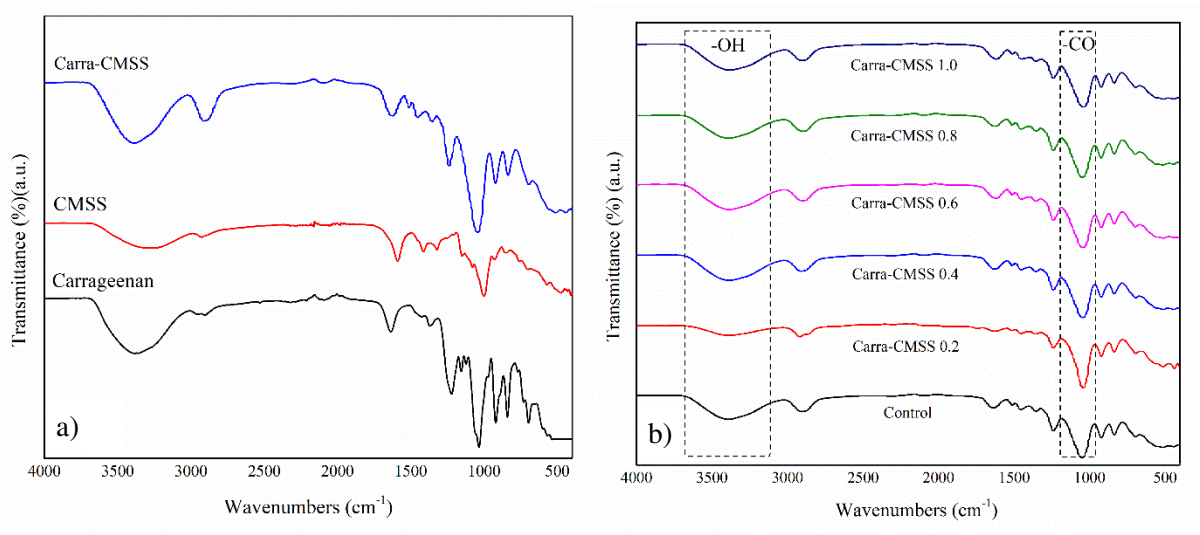

Figure 5. FTIR spectra of [a)]carrageenan, CMSS and Carra-HPMC/CMSS biocomposite films and [b)]Carra-HPMC/CMSS biocomposite films at different CMSS concentration.

3.4 Viscosity of Biocomposite and Mechanical Properties of the Biocomposite Films and Hard Capsules

Fig. 6 (a) depicts the relationship between viscosity and tensile strength of a film. The incorporation of CMSS in the carrageenan matrix gave a rise in viscosity with $p<0.05$ from 616.5 mPa·s to the highest value at Carra-CMSS 0.6 with 738.2 mPa·s. The increasing trend is proportional to the tensile strength, where the optimum was achieved at roughly the same CMSS concentration. The tensile strength was increased by 20.6% ($p<0.05$) from 51.2 MPa to 64.5 MPa after the addition of 0.4% CMSS. Similarly, Yusof [47] found that adding 5% CMSS to poly(L-lactide acid) (PLLA) nanofibres increased the tensile strength from 3.67 MPa to 9.34 MPa. The compaction of the composite structure contributes to the increase in film strength, which creates a more effective resistance against external load [48]. This is the result of blending efficiency that led to molecular arrangement via hydrogen bond formation. Moreover, the incorporation of carboxymethylated derivatives was reported to increase the film strength. This was presented by Suriyatem [49] who incorporated carboxymethyl chitosan to prepare rice starch films. The optimum point for capsule loop strength and elongation at break was achieved at the same CMSS concentration, which was 0.4% (Fig. 6 (b)). The capsule loop strength was increased by 7.7% ($p<0.05$) from 37.4 N to 40.5 N, and it could endure the applied pressure by up to 64.7%.

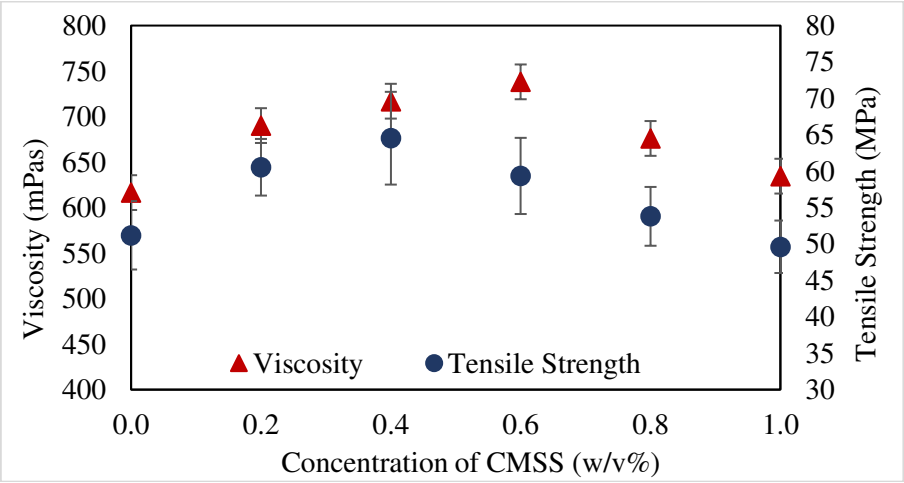

Figure 6(a). Effect of CMSS concentration on the viscosity and tensile strength of Carra-HPMC/CMSS biocomposite films.

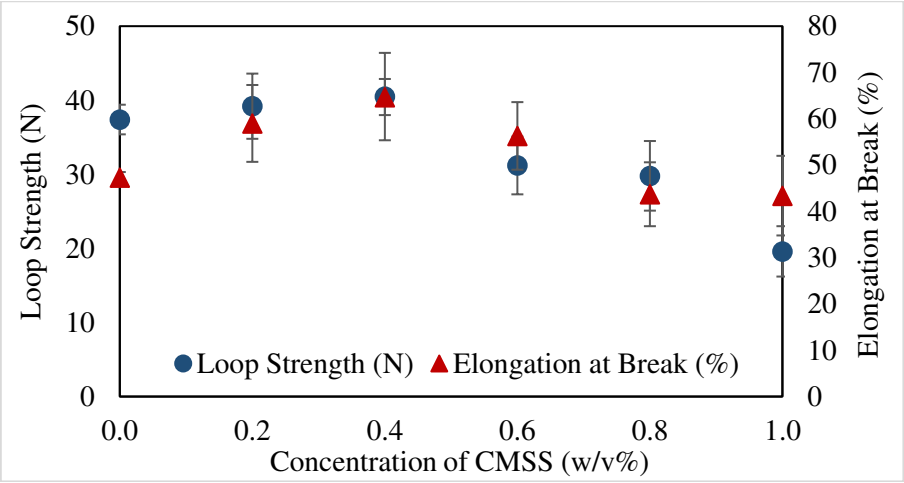

Figure 6(b). Effect of CMSS concentration on the elongation at break of Carra-HPMC/CMSS biocomposite films and loop strength of the hard capsules.

The mechanical strength decreased with a higher concentration of CMSS, up to 0.6%. Even at the highest viscosity, immiscibility due to CMSS agglomerates caused difficulty in proper mixing, resulting in non-uniform dispersion. Furthermore, the low molecular weight of CMSS compared to its native starch caused an increase in the molecular chain mobility, which reduced the tensile strength [50]. Stress concentration points also formed between the molecules, reducing the film elongation at break [51]. The optimised concentration of CMSS needs to be quantified in preparing hard capsules with the maximum ability to restrain the load applied for lower rejection rates during capsule filling.

Employing CMSS as a co-filler for carrageenan film was able to increase the mechanical properties, but only with a slight improvement compared to HPMC. In our previous work, HPMC could increase the film tensile strength and capsule loop strength of pure carrageenan by 59.1% and 46.9%, respectively. CMSS could not significantly increase the mechanical strength of the film due to limited capacity of the carrageenan film to hold both fillers within the matrix. Likewise, Wilpiszewska [50] reported that carboxymethyl cellulose (CMC)-based films exhibited notably better mechanical properties compared to the CMS-based films, which was due to the higher molecular weight of cellulose than starch derivatives.

3.5 Moisture Content and Disintegration Time of Carrageenan-HPMC/CMSS Biocomposite Films

Table 3 presents the moisture content and disintegration time of Carra-CMSS films. The moisture content of the film increased with $p<0.05$ as the CMSS concentration increased. The hydrophilicity of CMSS is the main factor that increases the amount of moisture in the film due to higher water absorption [47]. The increase in moisture content of starch film was also reported by Bodini [52], who compared the moisture in starch-HPMC film with different weight ratios. Carra-CMSS films up to 0.4% had a lower moisture content than the control carrageenan film. This shows that the complex film structure incorporated with fillers such as HPMC and CMSS could reduce the water permeability of the film. The moisture content must be controlled and comparable to that of commercial gelatin capsule with 13% moisture content [53]. Special attention must be paid to the drying method and storage conditions to produce starch hard capsules with lower moisture content, as these affect the physical and antifungal properties of the capsules [54].

Disintegration test evaluates a drug carrier's ability to disintegrate, allowing the active drug to be absorbed into the body. The higher the capsule's wetting rate or initial water absorption rate, the faster it will swell, resulting in a shorter disintegration time [55]. Table 4 shows that the control carrageenan hard capsule disintegrated the fastest, within 10.6 min, when compared to the composite hard capsule. The capsules with a higher molecular weight and viscosity dissolved slower because of greater entanglement and higher gel viscosity, as emphasised by Fu [56]. The best hard capsule based on mechanical properties, which was Carra-HPMC/CMSS 0.4, took 16.4 min to dissolve, exhibiting the shortest disintegration time, with $p<0.05$. Increasing CMSS concentration above 0.4% increased the disintegration time, which is related to the

reduction in capsule loop strength, as shown in Fig. 4(b). All samples, however, disintegrated within the time frame that satisfies the USP criteria for dietary supplement formulations, which is 30 minutes [57,58].

Table 3. Effect of CMSS concentration on the moisture content of Carra-HPMC/CMSS biocomposite films and disintegration time of hard capsules.

Samples	Moisture Content (%)	Disintegration Time (min)
Control	23.2 ± 2.8	10.6 ± 2.1
Carra-HPMC	14.6 ± 1.6	18.7 ± 1.8
Carra-HPMC/CMSS 0.2	18.0 ± 2.9	17.6 ± 2.3
Carra- HPMC/CMSS 0.4	20.9 ± 2.4	16.4 ± 1.0
Carra- HPMC/CMSS 0.6	25.4 ± 2.5	22.1 ± 2.4
Carra- HPMC/CMSS 0.8	29.6 ± 0.7	24.2 ± 2.0
Carra- HPMC/CMSS 1.0	31.3 ± 0.4	25.9 ± 0.5

3.6 Surface Morphology and Images of Carra-CMSS Biocomposite Films and Hard Capsules

The images in Fig. 7 present a comparison of film opacity prepared with different concentration of CMSS. The alphabet could be clearly seen through transparent biocomposite films with opacities less than 1.3%. A low opacity value corresponds to higher film transparency, and presents a homogeneous surface as observed at 3000x magnification using SEM. A uniform biocomposite without any phase separation demonstrates good compatibility between carrageenan and CMSS due to the same chemical unit which is glucose [39]. However, at 0.6% of CMSS, the alphabet was slightly blurred, whereas at 0.8% and 1.0% CMSS, visible irregularities and agglomerates of CMSS at the film surface could be observed. Excess CMSS in the carrageenan matrix led to higher light scattering and lower transmission through the film.

Figure 7. Images and surface morphology of Carra-HPMC/CMSS biocomposite films and hard capsules at different CMSS concentrations.

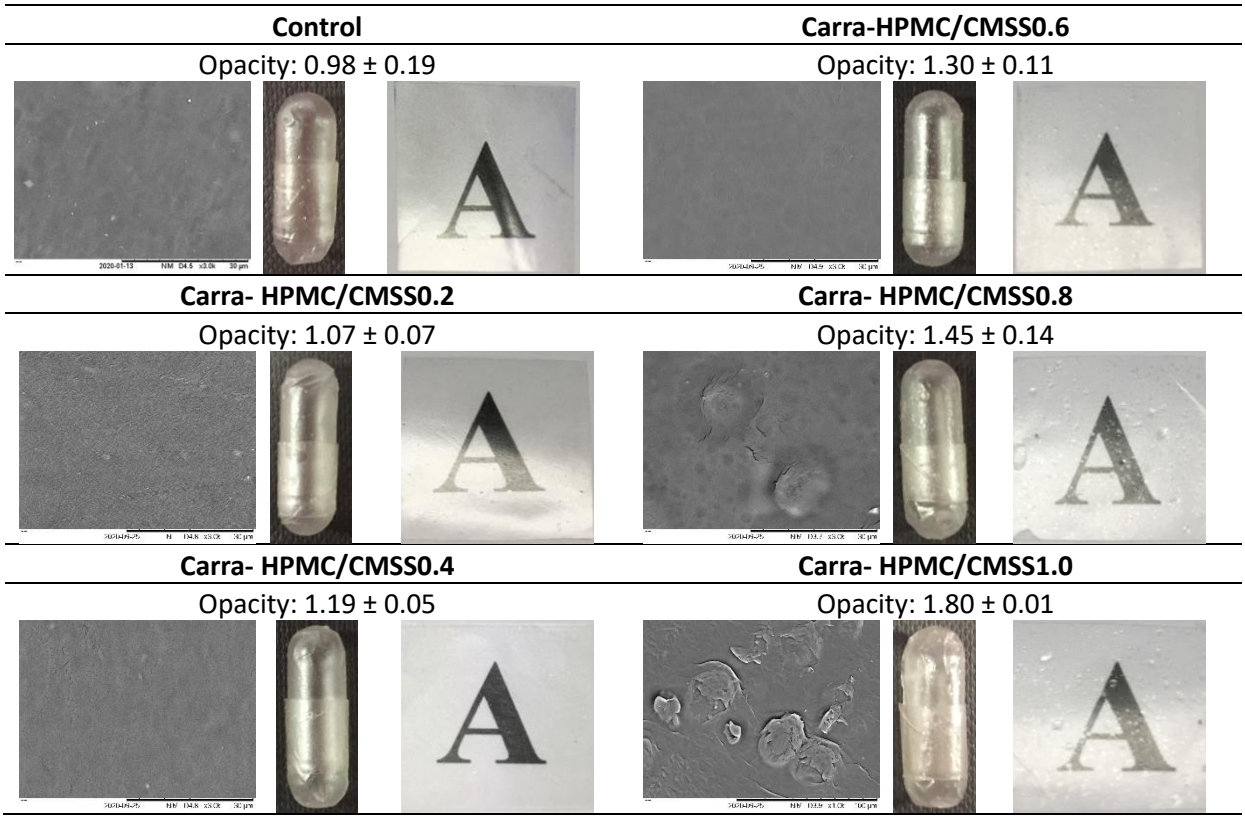

3.7 Thermal Analysis of Carra-CMSS Biocomposite Films

Carra-HPMC/CMSS0.4 film presented the best mechanical strength and was optically clear with no visible defects. Therefore, this film was chosen for subsequent thermal analysis in comparison to the control carrageenan film and Carra-HPMC film.

3.7.1 Differential Scanning Calorimetry Analysis

The thermal behaviour of control carrageenan, Carra-HPMC and Carra-HPMC/CMSS films was investigated and the thermograms of these films are displayed in Fig. 8. The glass transition temperature (T_g) of the control film was raised from 37.8°C to 47.8°C with CMSS contributing an additional 15.7% increment. The melting temperature (T_m) was also shifted from 65.4°C to 74.3°C with an additional 6.9% increment for Carra-HPMC/CMSS film, which indicated a chemical modification in the material. CMSS limits the mobility by reducing the free volume in the carrageenan matrix [59]. The exothermic transition at temperatures above 200°C was attributed to the pyrolysis of the methyl branches and the gas released by the system to shed heat. Carra-HPMC/CMSS presented the highest crystallisation temperature (T_c) at 276°C compared to the control carrageenan and Carra-HPMC with 238.0°C and 251.3°C, respectively. Table 4 summarises all transition temperatures and the enthalpy of melting and decomposition. Carra-HPMC/CMSS presented the highest thermal stability with improved T_g, T_m, and T_c. The inclusion of CMSS raised the enthalpy of melting transition (ΔH_m) by 5.6% from 180.8 J/g to 191.5 J/g, indicating that more energy was required to break the bond between molecules in the matrix [60]. In correlation to NMR and FTIR analysis, the intermolecular hydrogen bonding formed between the hydroxyl groups of carrageenan and CMSS increased the enthalpy, which then stabilised the biocomposite film.

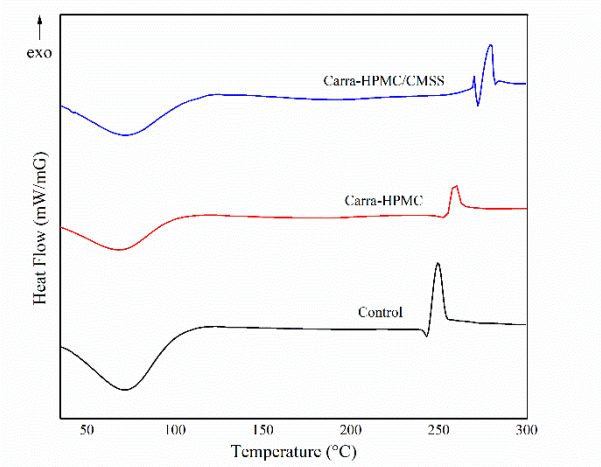

Figure 8. DSC thermograms of control, Carra-HPMC and Carra-HPMC/CMSS biocomposite films.

Table 4. Transition temperatures and enthalpies of control, Carra-HPMC and Carra-HPMC/CMSS biocomposite films.

Samples	T_g (°C)	T_m (°C)	ΔH_m (J/g)	T_c (°C)	ΔH_c (J/g)
Control	37.8	65.4	151.5	238.0	79.8
Carra-HPMC	40.3	69.2	180.8	251.3	52.9
Carra-HPMC/CMSS	47.8	74.3	191.5	276.9	73.2

3.7.2 Thermogravimetry Analysis

The thermal stability profiles of control, Carra-HPMC and Carra-HPMC/CMSS films are shown in Fig. 9. Polysaccharide samples generally exhibit three stages of thermal effect during thermal analysis [61]. The first stage is the degradation of volatile components, such as moisture, which occurs at temperatures lower than 100°C [16]. A steeper shoulder line at the first stage is observed for the control film due to its higher moisture content compared to others. The second stage is the decomposition of the carrageenan and the crosslinker, with maximum peaks at 200 to 450°C [12]. As shown in Fig. 9(a), the maximum weight

loss possessed by Carra-HPMC film was 30% at 225°C, which was delayed by 13.8% after the addition of CMSS. The temperature at which the highest weight loss for Carra-HPMC/CMSS film occurred was 261°C with 37%. The delay proved that the biocomposite film with added CMSS improves the thermal stability of carrageenan film. It was attributed to the high crosslinked structure and compact network of the biocomposite, which corresponded to the higher mechanical properties of Carra-HPMC/CMSS film. This improved the thermal stability, as shown in the DTG curve (Fig. 9(b)), where a higher temperature was required to decompose the film [20]. The decomposition of Carra-HPMC/CMSS was 3.2%/°C at 265.3°C, which was the highest compared to other films without CMSS. The thermogram results are summarized in Table 5, and these prove the positive effect of CMSS incorporation in thermally stabilising carrageenan biocomposite films to some degree.

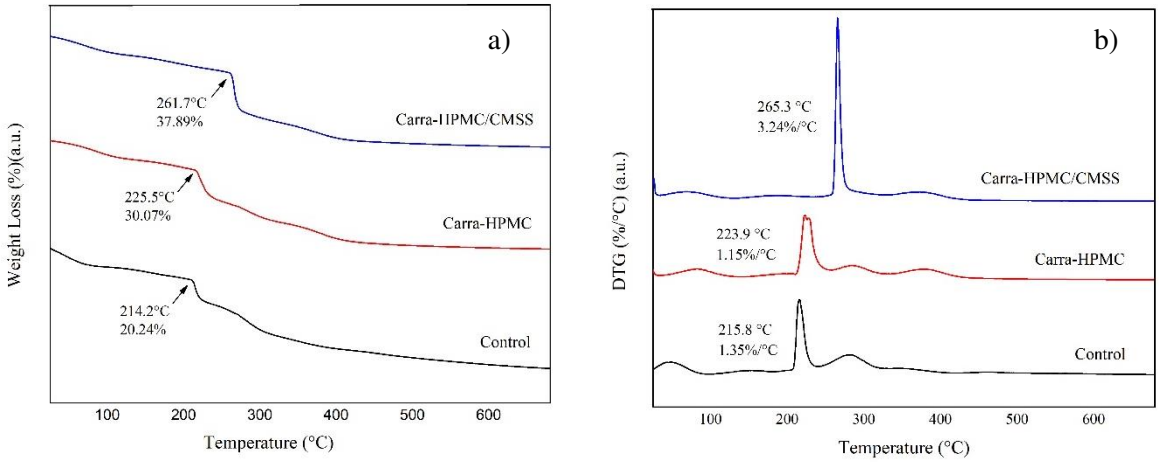

Figure 9. [a]TGA and [b]DTG thermograms of control, Carra-HPMC and Carra-HPMC/CMSS biocomposite films.

Table 5. Thermal degradation behaviour for control, Carra-HPMC and Carra-HPMC/CMSS biocomposite films.

Samples	Temperature Range (°C)	Weight Loss at Step End (%)	Temperature at Maximum Degradation Rate (°C)	Residues at 800°C (%)
Control	30-200	21.1	215.8	13.9
	200-700	65.0		
Carra-HPMC	30-200	19.4	223.9	22.9
	200-700	57.7		
Carra-HPMC/CMSS	30-200	20.3	265.3	21.3
	200-700	58.4		

3.8 Kinetic Analysis by Broido's Model

The activation energy (E_a) of control, Carra-HPMC and Carra-HPMC/CMSS films was calculated at temperatures ranging from 200 to 400°C, where the main decomposition of these films occurred, based on the TGA and DTG thermograms. E_a is the minimum energy required to break the bond between molecules in the surface of the substance during thermal degradation [62]. All results of E_a presented a good fit to depict the thermal degradation when applying the Broido's model, since high values of determination coefficient were achieved (R^2> 0.8) (Table 6). The E_a of the control film was 36.6 kJ·mol^{-1}, which was slightly higher than the values reported by Valenta [63], which ranged between 11.0 and 31.4 kJ·mol^{-1}. It is possible that the addition of crosslinker, plasticiser and toughening agent in the formulation stabilises the structure upon heating. The incorporation of HPMC increased the E_a by 33.3% to 54.9

kJ·mol^{-1}. A further increment by 26.2% was recorded after the addition of CMSS at optimised concentration, where the E_a was even higher, up to 74.4 kJ·mol^{-1}. This increment reflected its effect on the biocomposite film, which slowed down the decomposition process. The sample with the highest E_a indicates the highest resistance of its molecular structure to temperature [62,63]. This effect could be linked to the intermolecular hydrogen bonding formed between carrageenan and CMSS, as shown by NMR and FTIR. CMSS stabilised the molecular structure of the biocomposite, and subsequently improved the mechanical properties of the films and hard capsules.

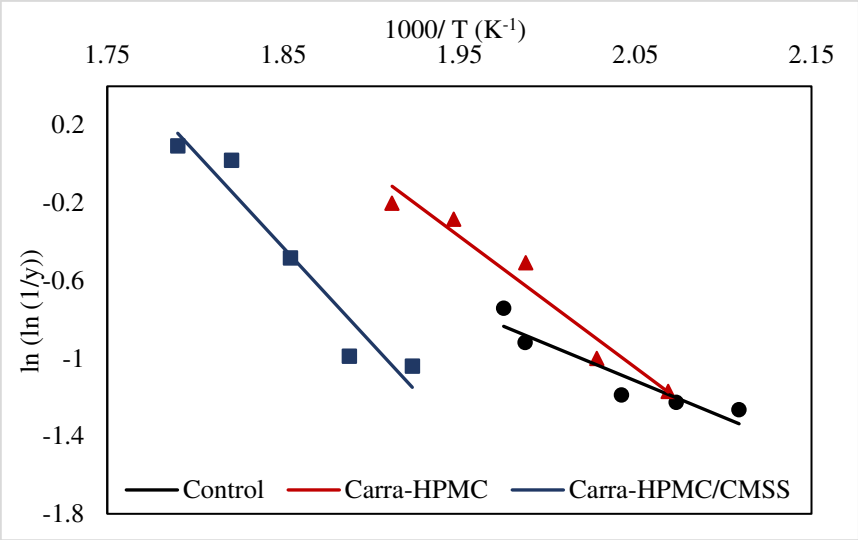

Figure 10. Graphical representation of Broido's plots for degradation of control, Carra-HPMC and Carra-HPMC/CMSS biocomposite films.

Table 6. Kinetic parameters of thermal degradation by Broido's model. Activation energy (E_a), Arrhenius constant (A) and coefficient of determination (R^2).

Samples	E_a (kJ·mol^{-1})	A	R^2
Control	36.6	7.8 x 10^3	0.8179
Carra-HPMC	54.9	3.6 x 10^5	0.9512
Carra-HPMC/CMSS	74.4	1.1 x 10^7	0.8310

4 Conclusion

The DFT calculations and ^{1}H NMR spectra established the intermolecular interaction between carrageenan and CMSS via hydrogen bonding and it was supported by FTIR result. The strong interaction between these two materials increased the mechanical strength of the carrageenan biocomposite film and hard capsule. Additionally, the increase of activation energy of the biocomposite film proves the enhanced thermal stability upon decomposition. However, methods on drying and sample storage need to be investigated further to reduce the high moisture content of Carra-HPMC/CMSS biocomposite. It is prone to humidity from its surroundings due to the hydrophilicity of CMSS. In spite of that, the improved mechanical and thermal properties of carrageenan biocomposite with CMSS incorporation, as reported, demonstrates the potential to be a hard capsule material replacing gelatin in the future.

Acknowledgements

The authors would like to thank the Ministry of Higher Education for providing financial support under Fundamental Research Grant Scheme (FRGS) No. FRGS/1/2019/TK05/UMP/02/2 (University reference RDU1901111) and Universiti Malaysia Pahang for laboratory facilities as well as additional financial support under Internal Research grant PGRS2003131.

Conflict of Interest Statement

The authors have declared no conflict of interest.

Symbols used

E_a	[kJ·mol^{-1}]	Activation energy
ΔH_m	[J/g]	Enthalpy of melting transition
ΔH_c	[J/g]	Enthalpy of crystallisation transition
T	[K]	Temperature
T_c	[°C]	Crystallisation temperature
T_g	[°C]	Glass transition temperature
T_m	[°C]	Melting temperature
R	[J·mol^{-1}·K^{-1}]	Universal gas constant
R^2	[-]	Determination coefficient
w_t	[µg]	Weight at any time
w_o	[µg]	Initial weight
w_∞	[µg]	Weight of residue
y	[-]	Degree of conversion

Greek letters

δ	[ppm]	Chemical shift

Sub- and Superscripts

D_2O	Deuterated water
^1H	Hydrogen-1 (proton) nuclei
H_i	Null analysis
H_o	Alternate analysis

Abbreviations

A	Pre-exponential factor
Abs	Absorbance
ATR-FTIR	Attenuated total reflectance - fourier transform infrared spectroscopy
b	Film thickness
Carra	Carrageenan
CMC	Carboxymethyl cellulose
CMS	Carboxymethyl starch
CMSS	Carboxymethyl sago starch
DA	4-linked 3,6-anhydro-α-D-galactopyranose
DFT	Density functional theory

DTG	Derivative thermogravimetry
G	Alternating 3-linked β-D-galactopyranose
H	Hydrogen atom
HPMC	Hydroxypropylmethyl cellulose
MESP	Molecule electronic surface potential
NMR	Nuclear magnetic resonance
O	Oxygen atom
OH	Hydroxide
PEG	Polyethylene glycol
PLLA	Poly(L-lactide acid)
SEM	Scanning electron microscopy
TGA	Thermogravimetry analysis

References

[1] B. Rabadiya, *Pharm. Res. Bio-Science* **2013**, *2*, 42.

[2] Adam F., Hamdan M. A., Abu Bakar S. H, 'Carrageenan : A Novel and Future Biopolymer', *Industrial Applications of Biopolymers and their Environmental Impact*, CRC Press **2020**, Vol. 31, p. 225.

[3] E. N. Dewi, Y. Darmanto, Ambariyanto, *J. Coast. Dev.* **2012**, *16*, 25.

[4] M. Rincón-Iglesias, E. Lizundia, C. M. Costa, S. Lanceros-Méndez, *ACS Appl. Polym. Mater.* **2020**, *2*, 1448.

[5] M. A. Hamdan, K. N. M. Amin, R. Jose, D. Martin, F. Adam, *Food Hydrocoll. Heal.* **2021**, 100023.

[6] B. Rukmanikrishnan, S. K. Rajasekharan, J. Lee, S. Ramalingam, J. Lee, *Mater. Today Commun.* **2020**, *24*, 101346.

[7] A. Farahnaky, R. Azizi, M. Majzoobi, G. Mesbahi, N. Maftoonazad, *Innov. Food Sci. Emerg. Technol.* **2013**, *20*, 173.

[8] W. A. Wan Yahaya, S. D. Subramaniam, N. A. Mohd Azman, F. Adam, M. P. Almajano, *Chem. Eng. Technol.* **2022**, *In Press*.

[9] M. A. Hamdan, N. A. Ramli, N. A. Othman, K. N. Mohd Amin, F. Adam, *Mater. Today Proc.* **2021**, *42*, 56.

[10] F. Adam, N. A. Othman, N. Hidayah, M. Yasin, C. K. Cheng, N. A. Mohd, *Fibers Polym.* **2022**.

[11] F. Adam, M. A. Hamdan, S. Hana, A. Bakar, M. Yusoff, R. Jose, *Chem. Eng. Commun.* **2020**, *208*, 741.

[12] F. Adam, J. Jamaludin, S. H. Abu Bakar, R. Abdul Rasid, Z. Hassan, *Cogent Eng.* **2020**, *7*.

[13] N. H. Zainal Abedin, A. H. Abu Bakar, *Int. J. Biol. Macromol.* **2018**, *114*, 710.

[14] H. P. S. Abdul Khalil, W. Y. Suk, F. A. T. Owolabi, M. K. M. Haafiz, M. R. Fazita, A. G. Deepu, M. Hasan, R. Samsul, *J. Phys. Sci.* **2019**, *30*, 23.

[15] N. A. Othman, F. Adam, N. H. Mat Yasin, *Mater. Today Proc.* **2020**, *41*, 77.

[16] S. K. Owusu-Ware, J. S. Boateng, B. Z. Chowdhry, M. D. Antonijevic, *Int. J. Pharm. X* **2019**, *1*, 100033.

[17] M. M. Al-Tabakha, *J. Pharm. Pharm. Sci.* **2010**, *13*, 428.

[18] E. Sanchez-Rexach, T. G. Johnston, C. Jehanno, H. Sardon, A. Nelson, *Chem. Mater.* **2020**, *32*, 7105.

[19] H. Mohamad Naim, A. N. Yaakub, D. A. Awang Hamdan, *Int. J. Agron.* **2016**, *2016*.

[20] Z. Jamingan, M. B. Ahmad, K. Hashim, N. Zainuddin, **2015**, *19*, 503.

[21] N. M. Kanafi, N. A. Rahman, N. H. Rosdi, *Mater. Today Proc.* **2019**, *7*, 721.

[22] M. Pooresmaeil, H. Namazi, *Carbohydr. Polym.* **2021**, *258*, 117654.

[23] S. Ezan, S. Z. Abidin, F. Adam, *Aust. J. Basic Appl. Sci.* **2017**, *11*, 176.
[24] M. S. Rahman, M. S. Hasan, A. S. Nitai, S. Nam, A. K. Karmakar, M. S. Ahsan, M. J. A. Shiddiky, M. B. Ahmed, *Polymers (Basel).* **2021**, *13*.
[25] N. A. Ramli, F. Adam, K. N. Mohd Amin, M. N. Adibi, M. E. Ries, *Can. J. Chem. Eng. Manuscr.* **2022**, *In Press*.
[26] P. Charisiadis, V. G. Kontogianni, C. G. Tsiafoulis, A. G. Tzakos, M. Siskos, I. P. Gerothanassis, *Molecules* **2014**, *19*, 13643.
[27] B. Liu, J. Li, W. Zeng, W. Yang, H. Yan, D. C. Li, Y. Zhou, X. Gao, Q. Zhang, *Chem. Mater.* **2021**, *33*, 580.
[28] S. Zhou, X. Zheng, X. Yu, J. Wang, J. Weng, X. Li, B. Feng, M. Yin, *Chem. Mater.* **2007**, *19*, 247.
[29] S. H. Abu Bakar, F. Adam, *Malaysian J. Anal. Sci.* **2017**, *21*, 979.
[30] M. I. Socaciu, M. Fogarasi, C. A. Semeniuc, S. A. Socaci, M. A. Rotar, V. Mureşan, O. L. Pop, D. C. Vodnar, *Polymers (Basel).* **2020**, *12*, 1.
[31] Ricardo Rodrigo Ramos Cecci, Adriano Alves Passos, Nathan Riany Valério Albino, Daniel da Silva Vicente, Ademir Severino Duarte, Maria Inês Bruno Tavares, *J. Mater. Sci. Eng. B* **2020**, *10*.
[32] M. Khalil, F. Z. Alqahtany, *J. Inorg. Organomet. Polym. Mater.* **2020**, *30*, 3750.
[33] M. Ganesan, S. Paranthaman, *J. Mol. Model.* **2021**, *27*, 1.
[34] L. Youssouf, L. Lallemand, P. Giraud, F. Soulé, A. Bhaw-Luximon, O. Meilhac, C. L. D'Hellencourt, D. Jhurry, J. Couprie, *Carbohydr. Polym.* **2017**, *166*, 55.
[35] P. Nonsuwan, K. Matsumura, *ACS Appl. Polym. Mater.* **2019**, *1*, 286.
[36] M. H. Abu Bakar, N. H. Azeman, N. N. Mobarak, M. H. H. Mokhtar, A. A. A. Bakar, *Polymers (Basel).* **2020**, *12*, 1.
[37] N. G. Voron'ko, S. R. Derkach, M. A. Vovk, P. M. Tolstoy, *Carbohydr. Polym.* **2017**, *169*, 117.
[38] M. Zdanowicz, T. Spychaj, *J. Appl. Polym. Sci.* **2014**, *131*, 9463.
[39] T. Jiang, Q. Duan, J. Zhu, H. Liu, L. Yu, *Adv. Ind. Eng. Polym. Res.* **2020**, *3*, 8.
[40] J. C. Chatham, S. J. Blackband, *ILAR J.* **2001**, *42*, 189.
[41] N. K. Zainuddin, A. S. Samsudin, *Mater. Today Commun.* **2018**, *14*, 199.
[42] K. Postolović, B. Ljujić, M. M. Kovačević, S. Đorđević, S. Nikolić, S. Živanović, Z. Stanić, *Mater. Today Commun.* **2022**, *31*.
[43] A. M. Ili Balqis, M. A. R. Nor Khaizura, A. R. Russly, Z. A. Nur Hanani, *Int. J. Biol. Macromol.* **2017**, *103*, 721.
[44] G. Sun, T. Liang, W. Tan, L. Wang, *Food Hydrocoll.* **2018**, *85*, 61.
[45] N. A. Nordin, N. A. Rahman, N. Talip, N. Yacob, *Macromol. Symp.* **2018**, *382*, 1.
[46] S. Roy, H. J. Kim, J. W. Rhim, *ACS Appl. Polym. Mater.* **2021**, *3*, 1060.
[47] M. R. Yusof, R. Shamsudin, Y. Abdullah, F. Yalcinkaya, N. Yaacob, *Polym. Adv. Technol.* **2018**, *29*, 1843.
[48] M. Asrofi, H. Abral, A. Kasim, A. Pratoto, M. Mahardika, F. Hafizulhaq, *Fibers* **2018**, *6*, 1.
[49] R. Suriyatem, R. A. Auras, P. Rachtanapun, *Ind. Crops Prod.* **2018**, *122*, 37.
[50] K. Wilpiszewska, A. K. Antosik, B. Schmidt, J. Janik, J. Rokicka, *Polymers (Basel).* **2020**, *12*, 1.
[51] C. Zhang, G. Sun, L. Cao, L. Wang, *Food Hydrocoll.* **2020**, *108*, 106012.
[52] R. B. Bodini, J. das G. L. Guimarães, C. A. Monaco-Lourenço, R. Aparecida de Carvalho, *J. Drug Deliv. Sci. Technol.* **2019**, *51*, 403.
[53] A. M. Smith, L. Grover, Y. Perrie, **2010**.
[54] R. Ghadermazi, S. Hamdipour, K. Sadeghi, R. Ghadermazi, A. Khosrowshahi Asl, *Food Sci. Nutr.* **2019**, *7*, 3363.
[55] B. Yang, C. Wei, Y. Yang, Q. Wang, S. Li, *Drug Dev. Ind. Pharm.* **2018**, *44*, 1417.
[56] M. Fu, J. Blechar, A. Sauer, J. Al-Gousous, P. Langguth, *Pharmaceutics* **2020**, *12*, 1.
[57] N. Hassan, T. Ahmad, N. M. Zain, *J. Food Sci.* **2018**, *83*, 2903.
[58] N. Glube, L. Von Moos, G. Duchateau, *Elsevier* **2013**, *3*, 1.
[59] A. Aydogdu, G. Sumnu, S. Sahin, *Carbohydr. Polym.* **2018**, *181*, 234.
[60] S. C. Joshi, **2011**, 1861.
[61] B. B. Sedayu, M. J. Cran, *Polymers (Basel).* **2020**, *12*, 1145.
[62] J. Jamaludin, F. Adam, R. A. Rasid, Z. Hassan, *Chem. Eng. Res. Bull.* **2017**, *19*, 80.
[63] T. Valenta, B. Lapčíková, L. Lapčík, *Colloids Surfaces A Physicochem. Eng. Asp.* **2018**, *555*, 270.

Table and Figure captions

Table 1 The calculated energies and enthaplies of raw and complex molecular structure of κ-carrageenan-CMSS.

Table 2. ^{1}H NMR chemical shifts of Carra-CMSS biocomposite.

Table 3. Effect of CMSS concentration on the moisture content of Carra-HPMC/CMSS biocomposite films and disintegration time of hard capsules.

Table 4. Transition temperatures and enthalpies of control, Carra-HPMC and Carra-HPMC/CMSS biocomposite films.

Table 5. Thermal degradation behaviour for control, Carra-HPMC and Carra-HPMC/CMSS biocomposite films.

Table 6. Kinetic parameters of thermal degradation by Broido's model. Activation energy (E_a), Arrhenius constant (A) and coefficient of determination (R^2).

Figure 1 Schematic representation of the preparation of Carra-CMSS biocomposite and the proposed hydrogen bonding interaction between both materials.

Figure 2 Optimized MESP structure of (a) κ -carrageenan and (b) CMSS.

Figure 3 Complex molecular structure of κ-carrageenan-CMSS conjugate.

Figure 4(a) ^{1}H-NMR spectrum of pure carrageenan.

Figure 4(b). ^{1}H-NMR spectrum of pure CMSS.

Figure 4(c). ^{1}H-NMR spectra of Carra-CMSS biocomposite.

Figure 5. FTIR spectra of $^{a)}$carrageenan, CMSS and Carra-HPMC/CMSS biocomposite films and $^{b)}$Carra-HPMC/CMSS biocomposite film at different CMSS concentrations.

Figure 6(a). Effect of CMSS concentration on the viscosity and tensile strength of Carra-HPMC/CMSS biocomposite films.

Figure 6(b). Effect of CMSS concentration on the elongation at break of Carra-HPMC/CMSS biocomposite films and loop strength of the hard capsules.

Figure 7. Images and surface morphology of Carra-HPMC/CMSS biocomposite films and hard capsules at different CMSS concentrations.

Figure 8. DSC thermograms of control, Carra-HPMC and Carra-HPMC/CMSS biocomposite films.

Figure 9. $^{(a)}$TGA and $^{(b)}$DTG thermograms of control, Carra-HPMC and Carra-HPMC/CMSS biocomposite films.

Figure 10. Graphical representation of Broido's plots for degradation of control, Carra-HPMC and Carra-HPMC/CMSS biocomposite films.

Entry for the Table of Contents

Research Article: Carrageenan hard capsules are being proposed as the alternative to gelatin. Herein, carboxymethyl sago starch (CMSS) was used as an excipient in the biocomposite for hard capsule production. The blending created hydrogen bond interactions between carrageenan and CMSS, which improved the mechanical and

Mechanical and Thermal Evaluation of Carrageenan Hard Capsule Incorporated with Starch Corroborated by DFT Calculations and 1H NMR Analysis

Nur Amalina Ramli, Fatmawati Adam*, Khairatun Najwa Mohd Amin, Noor Fitrah Abu Bakar, Michael E. Ries

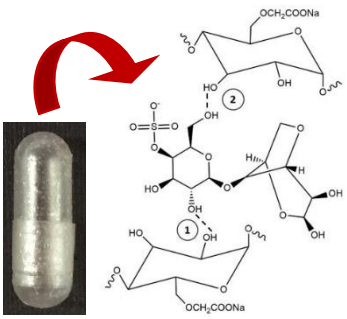

thermal properties of the hard capsule.